Am J Cancer Res 2025;15(5):2097-2110
www.ajcr.us /ISSN:2156-6976/ajcr0164671

Original Article

A long-lasting PI3Kδ inhibitor zandelisib forms a water-shielded hydrogen bond with p110δ and demonstrates sustained inhibitory effects

Kana Kunieda*, Chisae Nagiri*, Miwa Watanabe, Tadashi Yoshida, Jian Zou, Ayumi Kaneda, Yuichi Takahashi, Kenichi Aburai, Jun-Ichi Saito, Hiroshi Umehara, Yoshiaki Otsu, Toshihiko Ishii

*Research Division, Kyowa Kirin Co., Ltd., 1188, Shimotogari, Nagaizumi-cho, Sunto-gun, Shizuoka, Japan. *Equal contributors.*

Received March 20, 2025; Accepted May 4, 2025; Epub May 15, 2025; Published May 30, 2025

Abstract: Phosphatidylinositol 3-kinase isoform δ (PI3Kδ) phosphorylates phosphatidylinositol lipids, activating the AKT signaling pathway, which is crucial for essential cellular functions in B cells. Zandelisib, a selective PI3Kδ inhibitor, is under clinical development for treating B cell malignancies. Its intermittent dosing regimen sustains therapeutic effects while minimizing adverse effects. We explored zandelisib's pharmacological activity, focusing on its long-lasting property as a PI3Kδ inhibitor. To gain mechanistic insights, we compared the crystal structure of PI3Kδ in complex with zandelisib with other PI3K inhibitors. The binding kinetics of zandelisib, parsaclisib, idelalisib, and duvelisib to PI3Kδ were evaluated using surface plasmon resonance (SPR) analysis with the Biacore™ system, and their binding in living cells was confirmed using the NanoBRET™ TE Intracellular Kinase Assay system. We assessed the effects of drug wash-out on intracellular drug concentrations, AKT phosphorylation inhibitory activity, and cell growth inhibitory activity in SU-DHL-6 or WSU-FSCCL B cell lymphoma cell lines. Pharmacokinetics/pharmacodynamics analysis and anti-tumor activity evaluation were performed in mice bearing SU-DHL-6 tumors. The binding mode of zandelisib to PI3Kδ was revealed by X-ray crystallography. SPR analysis showed that zandelisib had a slower dissociation rate than other compounds, which was confirmed in cell-based binding assays. Idelalisib, parsaclisib, and duvelisib lost their PI3Kδ inhibitory activity by wash-out and showed a decreased cell growth inhibitory activity. In comparison, zandelisib exhibited sustained inhibitory activity against PI3Kδ and showed a more gradual decrease in cell growth inhibitory activity. Drug concentration after wash-out was highest for zandelisib. *In vivo* experiments using SU-DHL-6 tumor-bearing mice found zandelisib sustained PI3Kδ inhibitory effects for 8 hours at 50 mg/kg and 24 hours at 100 mg/kg. These results reflected significant anti-tumor activity of zandelisib in the B cell lymphoma model. The crystal structure of PI3Kδ in complex with zandelisib was determined at 2.5 Å resolution, revealing the benzimidazole group in zandelisib formed a hydrogen bond to the side chain of Lys779 in p110δ, the catalytic subunit of PI3Kδ. These studies demonstrated a longer duration of action of zandelisib compared to the other compounds, which was attributable to the hydrogen bond between zandelisib and Lys779 in p110δ.

Keywords: PI3Kδ, selective PI3Kδ inhibitor, AKT signaling pathway, crystal structure of PI3Kδ, hydrogen bond

Introduction

The mammalian class I phosphatidylinositol 3-kinases (PI3Ks) family is consisted of four members, PI3Kα, PI3Kβ, PI3Kγ, and PI3Kδ, which are composed of a heterodimer between a p110 catalytic subunit (p110α, p110β, p110γ, or p110δ) and a p85 regulatory subunit. Upon activation by stimuli, PI3Ks activate the AKT signaling pathways [1]. PI3Kδ plays a crucial role in various essential cellular functions in B cells, such as cell growth, proliferation, metabolic processes, migration, and additional important biological functions [2-4].

Up to now, PI3Kδ emerged as a potential target for drug development, especially in inflammatory diseases and hematological cancers. PI3Kδ inhibitors have shown efficacy in the treatment of chronic lymphocytic leukemia (CLL), non-Hodgkin's lymphoma (NHL) and other types of lymphoma [5-7]. However, while showing efficacy, it has also been reported that PI3Kδ inhibitors caused toxicities such as diarrhea/colitis,

https://doi.org/10.62347/JCGQ1004

pneumonitis, neutropenia, elevated serum aminotransferase levels, and so on [8]. These toxicities are mostly considered to be on-target and immune-mediated. Although several PI3Kδ inhibitors have been approved by the Food and Drug Administration (FDA), their clinical application has been limited due to severe adverse effects. At the Oncologic Drugs Advisory Committee meeting of the FDA in April 2022, safety concerns and regulatory considerations surrounding PI3Kδ inhibitors in hematologic malignancies were discussed, resulting in the withdrawal of application for several indications [9, 10].

Zandelisib (PWT143, ME-401) is a selective inhibitor of PI3Kδ. Zandelisib inhibits PI3Kδ-mediated AKT phosphorylation and TNFα release in human B cell lymphoma Raji cells cultured with anti-IgM, and expression of CD63 on primary basophils activated by anti-IgE. Zandelisib also demonstrates inhibitory effects on the growth of primary B cell malignancies [11, 12]. Initial results from a dose-escalation study of zandelisib in patients with relapsed/refractory follicular lymphoma and CLL/small lymphocytic lymphoma indicated that zandelisib was well tolerated and showed high response rates. Furthermore, when the intermittent dosing regimen of zandelisib (days 1-7 on, days 8-28 off) was compared with continuous dosing regimen in the study, it was revealed that the intermittent dosing regimen had the potential to reduce toxicity while maintaining efficacy [13-16]. A preclinical study has shown that zandelisib binds to PI3Kδ protein with a slower dissociation rate compared to idelalisib and is easily transferred from blood to tumor, suggesting that such properties of zandelisib may contribute to the high and long-lasting clinical efficacy in B cell malignancies [17].

In the present study, to better understand the pharmacological activity of the zandelisib, especially the long-lasting property in PI3Kδ inhibition, we evaluated the PI3Kδ inhibitory activity of zandelisib *in vitro*, comparing with 3 PI3Kδ inhibitors, 2 commercial (idelalisib and duvelisib) and 1 under clinical investigation (parsaclisib). Of these, idelalisib and parsaclisib are PI3Kδ selective, while duvelisib is a dual inhibitor of PI3Kδ and PI3Kγ [18]. In addition, the relationship between drug concentration and PI3Kδ inhibiton was evaluated *in vitro* and *in vivo*. Furthermore, the co-crystal structure of the PI3Kδ in complex with zandelisib was determined by X-ray crystallography to understand the molecular mechanism of the prolonged binding to the enzyme protein.

Materials and methods

Compounds

Zandelisib was kindly provided by MEI Pharma Inc. (San Diego, CA, USA). Idelalisib, parsaclisib, duvelisib, and PI103 were obtained from MedChemExpress or Tokyo Medical Industry. Wortmannin was obtained from Sigma-Aldrich. For *in vitro* experiments, these compounds were prepared in dimethyl sulfoxide (DMSO) to a concentration of 10 mmol/L before use.

Purified enzyme-binding kinetics

PI3Kδ protein (Biotinylated PIK3CD/PIK3R1 from Carna Biosciences, Inc.) was diluted to 20 μg/mL in Biacore buffer (50 mmol/L Tris pH 7.5, 0.05 vol% Tween 80, 150 mmol/L NaCl, and 5 mmol/L $MgCl_2$), and immobilized on a Sensor Chip SA (Cytiva) through the biotin-tag. Remaining streptavidin was blocked with 10 μg/mL biocytin injections to circumvent nonspecific binding of compounds to the streptavidin-bound surface. To obtain a stable signal after compound and buffer injections, the experiment was started after running buffer (1 vol% DMSO in Biacore buffer) injections. Zandelisib, parsaclisib, idelalisib, and duvelisib were diluted to 100, 31.6, 10, 3.16, and 1 nmol/L with running buffer. The single cycle kinetic experiments were performed with a compound concentration gradient of 1-100 nmol/L, with a contact time of 100 sec and a flow rate of 30 μl/min. The dissociation period was 1800 sec. A sensorgram of each compound was created by the Biacore™ 8K control Software (Cytiva). The resulting sensorgram curve was fitted to the 1:1 binding model by the software. For each sensorgram, association rate constant (k_a), dissociation rate constant (k_d), and equilibrium dissociation constant (K_D) were calculated by the software. The values in duplicated experiments for each compound were geometrically averaged by Microsoft Excel for Microsoft 365 (version 2102).

Analysis of intracellular residence time on PI3Kδ

Residence time of each compound on PI3Kδ was measured using NanoBRET™ TE Intra-

cellular Kinase Assay, K-3 (Promega Corporation) according to the manufacturer's instruction [19]. Briefly, HEK293 cells (American Type Culture Collection (ATCC), CRL-1573) were transiently transfected with both a NanoLuc®-PIK-3CD Fusion Vector (Promega) and a PIK3R1 Expression Vector, with the purpose of reconstructing the complete PI3Kδ enzyme (Promega). The transfected cells were incubated with IC_{80} concentration of each compound (zandelisib: 1 nmol/L, parsaclisib: 10 nmol/L, idelalisib: 30 nmol/L, duvelisib: 30 nmol/L, and wortmannin: 100 nmol/L) for 2 hours (37°C, 5% CO_2). After the incubation, the cells were washed twice with medium, and then treated with NanoBRET™ Nano-Glo® Substrate solution and NanoBRET™ Tracer Reagent (Promega). Bioluminescence resonance energy transfer (BRET) signals were measured repeatedly with the GloMax® Discover Multimode Microplate Reader (Promega) under the following conditions; donor filter: 450 nm BP, acceptor filter: 600 nm LP, integration time: 0.3 s/well, measurement interval: 1.5 min, iteration: 81. The data was fitted to the kinetic equation [20], and the residence time (the reciprocal of dissociation rate constant) of each compound was estimated.

B cell lymphoma cell lines

The two human B cell lymphoma cell lines, SU-DHL-6 and WSU-FSCCL were purchased from ATCC (CRL-2959) and Leibniz Institute DSMZ-German Collection of Microorganisms and Cell Cultures GmbH (ACC612), respectively. The cells were cultured in RPMI 1640 medium (Thermo Fisher Scientific) supplemented with 10% fetal bovine serum (Thermo Fisher Scientific) and incubated at 37°C, 5% CO_2.

Measurement of AKT phosphorylation in a wash-out experiment

SU-DHL-6 cells at 1 × 10^6 cells/well in 6-well plate were exposed to culture medium containing vehicle, zandelisib, idelalisib, parsaclisib, or duvelisib at 10, 100, or 1000 nmol/L and incubated for 1, 23, or 24 hours. Subsequently, cells were washed twice with 5 mL of Dullbecco's phosphate-buffered saline (DPBS) and further incubated in culture medium lacking PI3Kδ inhibitors for 23, 1, or 0 hours such that the total time of drug exposure and wash-out was 24 hours. After 24 hours incubation, the cells were collected and stored at -80°C for measurement of AKT phosphorylation and intracellular compound concentration. Twenty μg of protein lysates were analyzed by SDS-PAGE under reducing and denaturing condition. Phospho-AKT Ser473 (p-AKT (Ser473)), phospho-AKT Thr308 (p-AKT (Thr308)), and β-actin were detected by Western Blotting. The following antibodies were used: Phospho-Akt (Ser473) (D9E) XP ® Rabbit mAb (Cell Signaling Technology), Phospho-Akt (Thr308) (244F9) Rabbit mAb (Cell Signaling Technology), Monoclonal Anti-beta-Actin antibody A5441 (Sigma-Aldrich), Anti-Rabbit IgG, HRP-Linked Whole Ab Donkey (GE Healthcare), and anti-mouse IgG, HRP-Linked Species-Specific whole antibody (from sheep) (GE Healthcare). Can Get Signal ® (Toyobo) was used for detection of p-AKT (Ser473 and Thr308).

Measurement of cell proliferation in a wash-out experiment

SU-DHL-6 and WSU-FSCCL cells were seeded in 384-well plates at 1000 cells/40 μL/well. Cells were exposed to test compounds at 0.1, 1, 10, 100, 1000, and 10000 nmol/L, and incubated for 1, 24, 48, 72, or 96 hours. Subsequently, cells were washed and further incubated in the absence of test compounds for 95, 72, 48, or 24 hours such that the total time of drug exposure and wash-out was 96 hours. Cells treated with the test compound for 96 hours were not subjected to the wash-out procedure. After 96 hours incubation, luminescence was measured by Cell Titer Glo Reagent (Promega) on an EnVision (Perkin Elmer).

In vivo studies in SU-DHL-6 xenograft model

Animal experiments were performed in an AAALAC-accredited institution. All animal studies were performed in accordance with company policy on the care and use of laboratory animals (Kyowa Kirin Co., Ltd., Shizuoka, Japan).

Male SCID mice were purchased from CLEA Japan, Inc. (Tokyo, Japan). In anti-tumor examination, SU-DHL-6 cells were suspended in DPBS containing 50 vol% matrigel and inoculated subcutaneously into the right flank region of 8-week-old male SCID mice at 1 × 10^7 cells/0.1 mL/mouse. On the day before tumor cell inoculation, the mice were given an intraperitoneal injection of anti-asialo GM1 anti-

body. Seventeen days after the inoculation, 30 mice were divided into two groups for vehicle and zandelisib (100 mg/kg) administration (n = 15). Zandelisib was prepared in 20% VE-TPGS + 80% 100 mmol/L citrate buffer (pH 3.5) and administrated orally. Administration was performed once daily from day 0 (the day of group allocation) to day 13. The experiments were terminated 2 weeks after the start of treatment. No animal reached the predetermined humane endpoint. Tumor volumes from day 0 were calculated as follows; tumor volume (mm^3) = DL × DS^2 × 0.5, (DL, long diameter, DS, short diameter). Difference of the tumor volumes on day 14 between vehicle and zandelisib groups was statistically analyzed by Aspin-welch test using the SAS software program (release 9.4, SAS Institute Inc.).

For pharmacokinetic analysis, SU-DHL-6 tumor-bearing SCID mice treated as described above were orally administered zandelisib at 50 or 100 mg/kg. Blood and tumor samples were collected from the mice at 0.5, 2, 8, 24, and 72 hours after administration of zandelisib at 50 mg/kg (n = 3), and at 0.25, 0.5, 2, 4, 8, 24, 48, and 72 hours after administration of zandelisib at 100 mg/kg (n = 4). Blood samples were centrifuged to obtain plasma samples. Plasma and tumor samples were stored frozen until use in the analysis.

Quantification of test compounds concentration

The concentration of zandelisib, idelalisib, parsaclisib, and duvelisibs in SU-DHL-6 cells prepared as described in "Measurement of AKT phosphorylation in a wash-out experiment" and concentration of zandelisib in the plasma and tumor sample prepared as described in "*in vivo* studies in SU-DHL-6 xenograft model" were determined by liquid chromatography tandem mass spectrometry (LC/MS/MS). Cell samples were homogenized with water using an ultrasonic homogenizer. Tumor samples were homogenized with saline using a shaking homogenizer. Protein was precipitated from the homogenate and plasma samples by the addition of acetonitrile (cell samples) or formic acid containing acetonitrile (plasma and tumor samples), and the extracts were subjected to LC/MS/MS analysis. As internal standards, warfarin was used for plasma and tumor samples and (±)-propranolol hydrochloride was used for cell samples. The analyte were separated on a C18 (cell samples) or C8 reverse-phase (plasma and tumor samples) columns. For ionization, electrospray in positive ionization mode (cell samples) or atmospheric pressure chemical ionization (APCI) in positive mode (plasma and tumor samples) was conducted. The detected *m/z* in cell samples for zandelisib, idelalisib, parsaclisib, or duvelisib were 577/230, 416/176, 433/150, 417/282 (Q1/Q3), respectively. The detected *m/z* in plasma and tumor samples was 577/348 (Q1/Q3) for zandelisib. The lower limit of quantification (LLOQ) for cell samples, plasma samples, and tumor samples were 0.0025 pmol/10^6 cells, 0.5 ng/mL, or 10 ng/g, respectively.

Structure determination of PI3Kδ in complex with zandelisib by X-ray crystallography

The complex of human p110δ (amino acids 1-1044) and bovine p85 (amino acids 431-600) was purchased from Proteros biostructures GmbH for the structural analysis. The crystals were prepared based on the previous papers [21]. In brief, the protein at a concentration of 6 mg/mL was incubated with zandelisib and crystallized by vapor diffusion in sitting drops at 10°C. Crystals were dehydrated manually using trimethylamine N-oxide as an osmolite and frozen in liquid nitrogen. X-ray diffraction data were collected at the Swiss Light Source (beamline PXII/X10SA). The PI3Kδ structure in complex with zandelisib was determined by molecular replacement using for known PI3Kδ structure (PDB ID: 6PYR) as a search model.

Results

Binding kinetics against PI3Kδ evaluated by the surface plasmon resonance analysis

The structures of the PI3K inhibitors used in this experiment are shown in **Figure 1**. Among these compounds, the binding kinetics of zandelisib, idelalisib, parsaclisib, and duvelisib against PI3Kδ were evaluated by the surface plasmon resonance (SPR) analysis using Biacore™ system (**Figure 2**). Binding parameters are summarized in **Table 1**. Zandelisib showed the longest residence time among the four compounds. After the first injection of each compound followed by a 1800-sec of dissociation period, the same compound was injected again, and the response was measured. No binding was observed in the second measure-

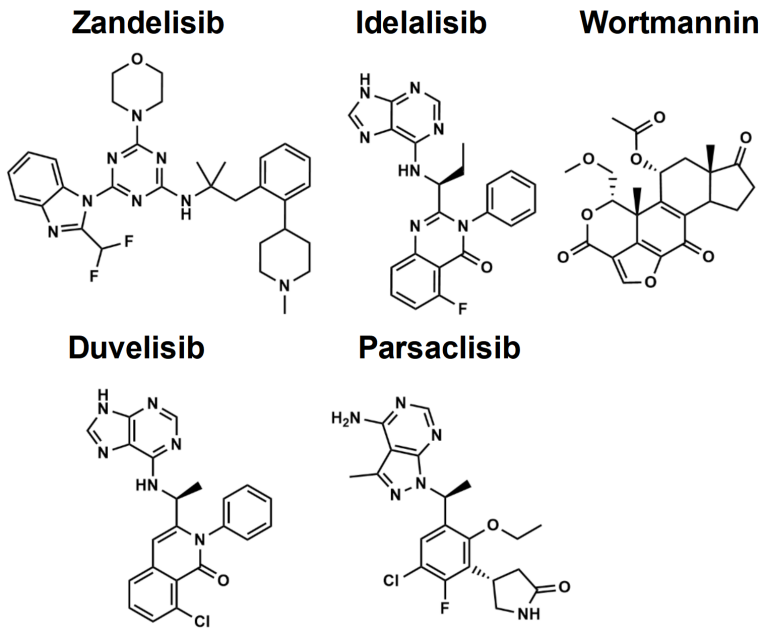

Figure 1. Chemical structures of select PI3K inhibitors.

ment of zandelisib (Supplementary Figure 1A), which indicated no dissociation of the first bound zandelisib. On the other hand, binding was observed again in the second injection of idelalisib, parsaclisib, or duvelisib (Supplementary Figure 1B-D), indicating that the first-bound compounds, idelalisib, parsaclisib, or duvelisib, had dissociated.

Analysis of binding kinetics against PI3Kδ in living cells

The binding of the test compounds to PI3Kδ in living cells was confirmed by NanoBRET™ TE Intracellular Kinase Assay system and the residence time of each compound was measured (**Figure 3**). Wortmannin, a covalent binder to PI3Kδ, was also evaluated in this assay. The residence time of each compound was 484.4, 20.2, 59.9, 158.2, and 228.2 minutes for zandelisib, idelalisib, parsaclisib, duvelisib, and wortmannin, respectively (**Table 2**). Among the five compounds examined, zandelisib showed the longest residence time.

Evaluation of drug wash-out effects on AKT phosphorylation inhibition

SU-DHL-6 cells were treated with the test compounds, washed, and further incubated in the absence of compounds. After a total incubation time of 24 hours, AKT phosphorylation was measured, and the effect of the drug-free period on the AKT phosphorylation was evaluated. Decreases of p-AKT (Ser473) and p-AKT (Thr308) were observed after 24 hours of continuous treatment (24 h-On) of all test compounds, suggesting that they all inhibited AKT phosphorylation (**Figure 4A**). AKT phosphorylation was also inhibited by 23-hour treatment of zandelisib followed by one-hour drug-free period (23 h-On/1 h-Off), although the inhibition level seemed weaker than 24 h-On. Furthermore, AKT phosphorylation was inhibited even by 1-hour treatment of zandelisib at 1000 nmol/L followed by 23-hour drug-free period (1 h-On/23 h-Off). Conversely, no inhibition of AKT phosphorylation was observed with the treatment of idelalisib, parsaclisib, or duvelisib in either the 23 h-On/1 h-Off or 1 h-On/23 h-Off schedules.

Determination of the intracellular concentration

The intracellular concentration of zandelisib, idelalisib, parsaclisib, and duvelisib in SU-DHL-6 cells treated with 1000 nmol/L of each compound, as described in "Evaluation of drug wash-out effects on AKT phosphorylation inhibition", were determined using LC/MS/MS (**Figure 4B**). Intracellular concentrations of zandelisib were the highest in all schedules compared to those of other compounds.

Evaluation of the effects of drug wash-out on cell viability of B cell lymphoma cell lines

SU-DHL-6 cells and WSU-FSCCL cells were treated with test compounds for 1, 24, 48, 72, or 96 hours and further incubated in the absence of each test compound for 95, 72, 48, 24, or 0 hours, respectively (1 h-On/95 h-Off, 24 h-On/72 h-Off, 48 h-On/48 h-Off, 72 h-On/24 h-Off, 95 h-On/1 h-Off, and 96 h-On). Cell viability was measured 96 hours after the initiation of treatment with the test compounds (**Figure 5**). The IC_{50} values for each compound under each condition are shown in (**Tables 3**,

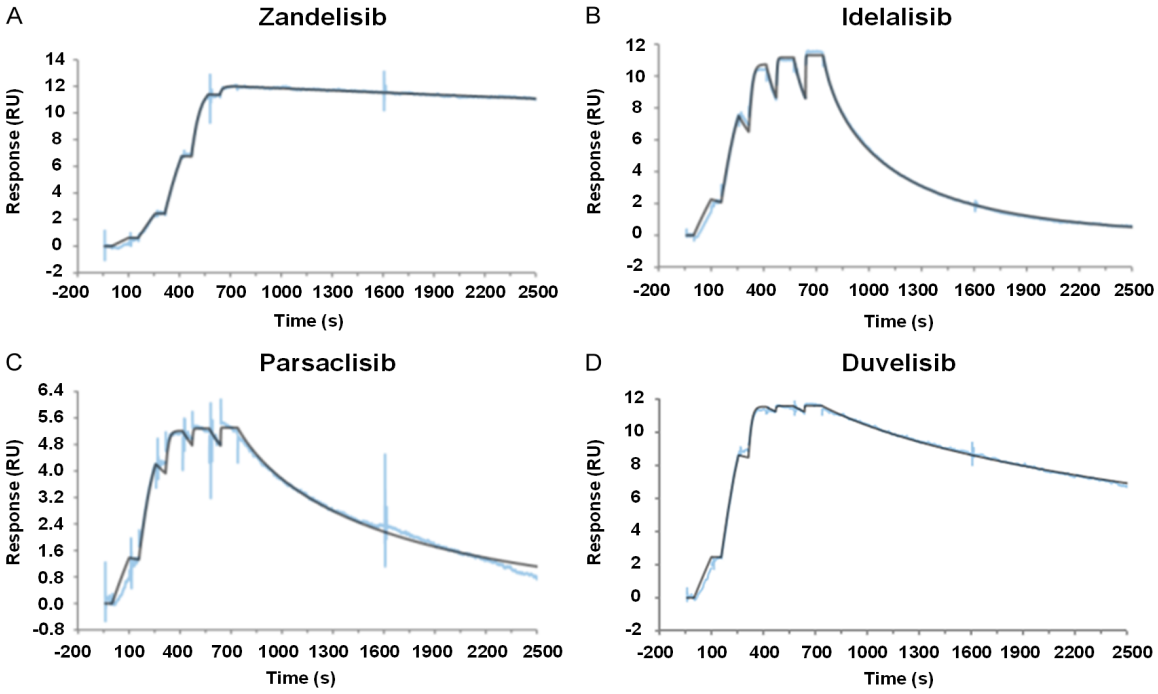

Figure 2. Single cycle kinetic curves of zandelisib, idelalisib, parsaclisib, or duvelisib on PI3Kδ. Single cycle kinetic assay of (A) 1-100 nmol/L zandelisib, (B) 1-100 nmol/L idelalisib, (C) 1-100 nmol/L parsaclisib, and (D) 1-100 nmol/L duvelisib on PI3Kδ was performed in duplicate. N = 1 data are shown. The blue line shows the sensorgram before fitting, and the black line shows the sensorgram after fitting using Biacore™ 8K control Software.

Table 1. Binding kinetics of zandelisib, idelalisib, parsaclisib, and duvelisib on PI3Kδ

Compound	k_a (1/M·s)	k_d (1/s)	K_D (M)	$t_{½}$ (s)	Residence time (s)
Zandelisib	7.74×10^5	3.96×10^{-5}	5.12×10^{-11}	17465	25239
Idelalisib	8.61×10^6	5.40×10^{-3}	6.27×10^{-10}	129	185
Parsaclisib	7.03×10^6	1.30×10^{-3}	1.85×10^{-10}	534	771
Duvelisib	9.79×10^6	4.79×10^{-4}	4.89×10^{-11}	1445	2086

The values in duplicated experiments for each compound were geometrically averaged. k_a: association rate constant, k_d: dissociation rate constant, K_D: equilibrium dissociation constant, $t_{1/2}$: half-life, s: second.

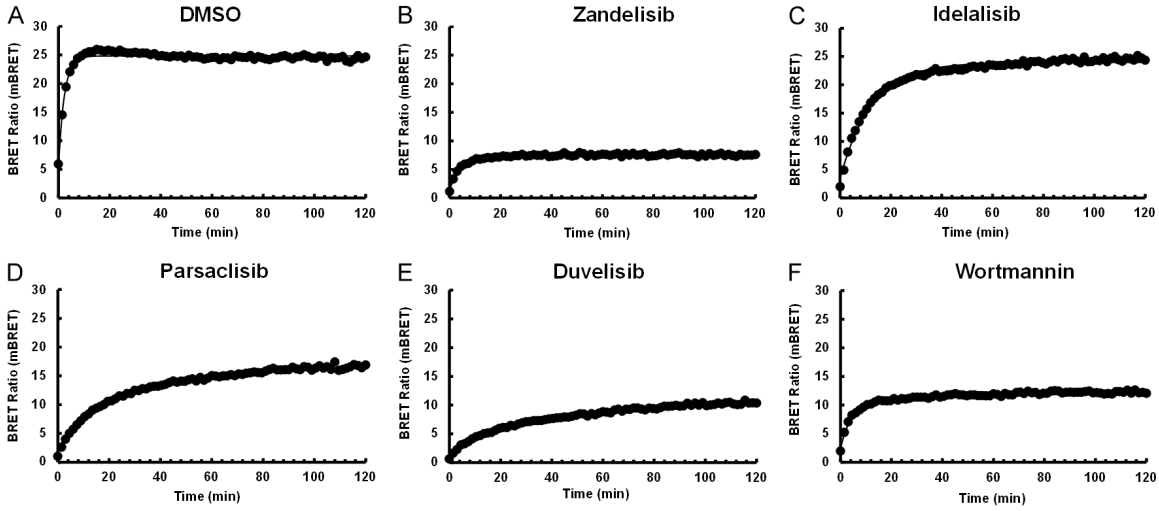

Figure 3. Residence time determination in HEK293 cells by NanoBRET™ assay. HEK293 cells were transfected with NanoLuc®-PIK3CD Fusion Vector and PIK3R1 Expression Vector. The cells were incubated with (A) DMSO, (B) zandelisib, (C) idelalisib, (D) parsaclisib, (E) duvelisib, or (F) wortmannin for 2 hours. After washing, the cells were treated with NanoBRET™ Nano-Glo® Substrate solution and NanoBRET™ Tracer Reagent, and the BRET signal was measured repeatedly. The X and Y axes represent the time after addition of NanoBRET™ Tracer Reagent and BRET signal, respectively. The value on Y axis stands for degree of replacement of each compound with NanoBRET™ Tracer, which means dissociation of each compound from PI3Kδ.

Table 2. Residence time of each compound

Compound	Zandelisib	Idelalisib	Parsaclisib	Duvelisib	Wortmannin
Residence time (min)	484.4	20.2	59.9	158.2	228.2

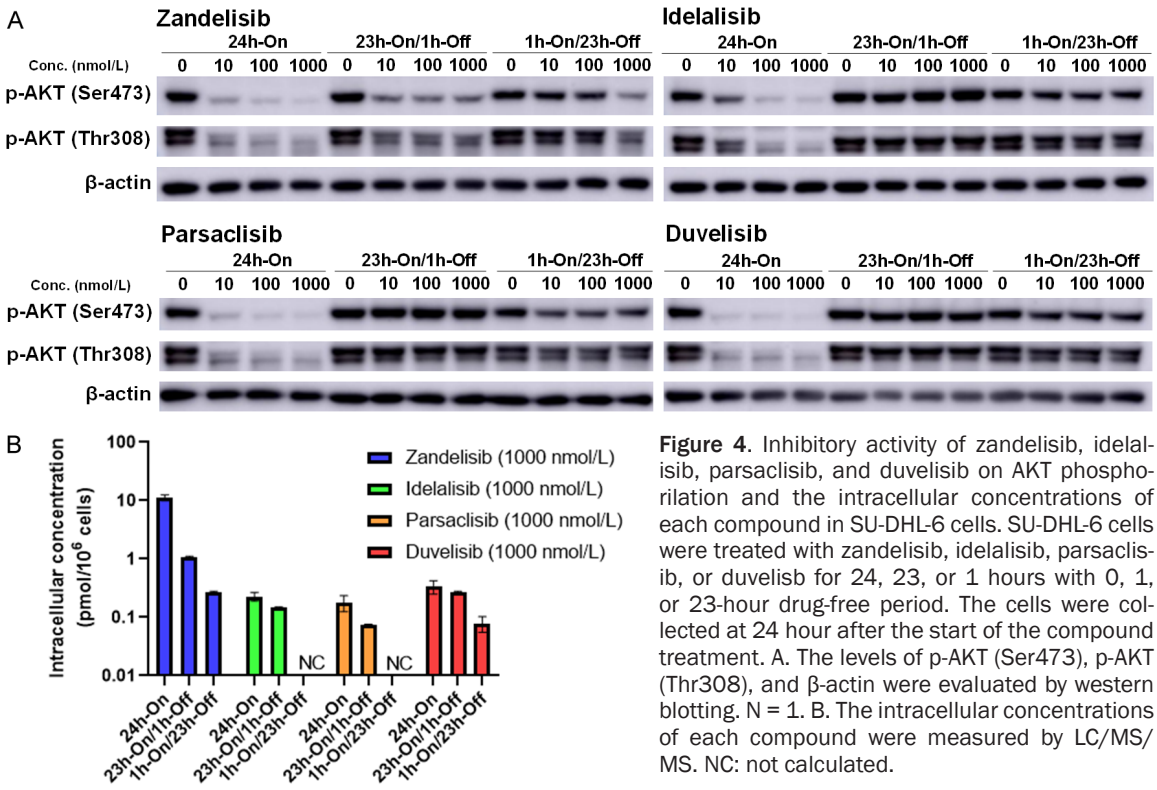

Figure 4. Inhibitory activity of zandelisib, idelalisib, parsaclisib, and duvelisib on AKT phosphorilation and the intracellular concentrations of each compound in SU-DHL-6 cells. SU-DHL-6 cells were treated with zandelisib, idelalisib, parsaclisib, or duvelisb for 24, 23, or 1 hours with 0, 1, or 23-hour drug-free period. The cells were collected at 24 hour after the start of the compound treatment. A. The levels of p-AKT (Ser473), p-AKT (Thr308), and β-actin were evaluated by western blotting. N = 1. B. The intracellular concentrations of each compound were measured by LC/MS/MS. NC: not calculated.

4). The inhibitory activity of all test compounds was attenuated by increasing drug-free period. However, the extent of the attenuation was least in zandelisib in both cell lines compared to the other test compounds.

Pharmacokinetics/pharmacodynamics and anti-tumor effects of zandelisib in SU-DHL-6 tumor-bearing mice

Pharmacokinetics/pharmacodynamics (PK/PD) relationships of zandelisib were investigated in the SU-DHL-6 s.c. xenograft model. In this study, zandelisib was orally dosed at 50 or 100 mg/kg. Zandelisib concentrations in plasma and tumor, expressions of p-AKT (Ser473), p-AKT (Thr308), and β-actin in tumor were evaluated at each time point and are indicated in **Figure 6**. The plasma and tumor concentration-time profiles of zandelisib are shown in **Figure 6A** and **6B**, while the PK parameters are shown in **Tables 5** and **6**. The concentration of zandelisib in the tumor was considerably higher than that in plasma at both doses, leading to higher C_{max} and AUC values in tumor than those in plasma. The relative levels of p-AKT (Ser473) and p-AKT (Thr308) were decreased at 0.5, 2, 4, 8, and 24 hours after administration of 100 mg/kg zandelisib. The Relative levels of p-AKT (Ser473) and p-AKT (Thr308) were also de-

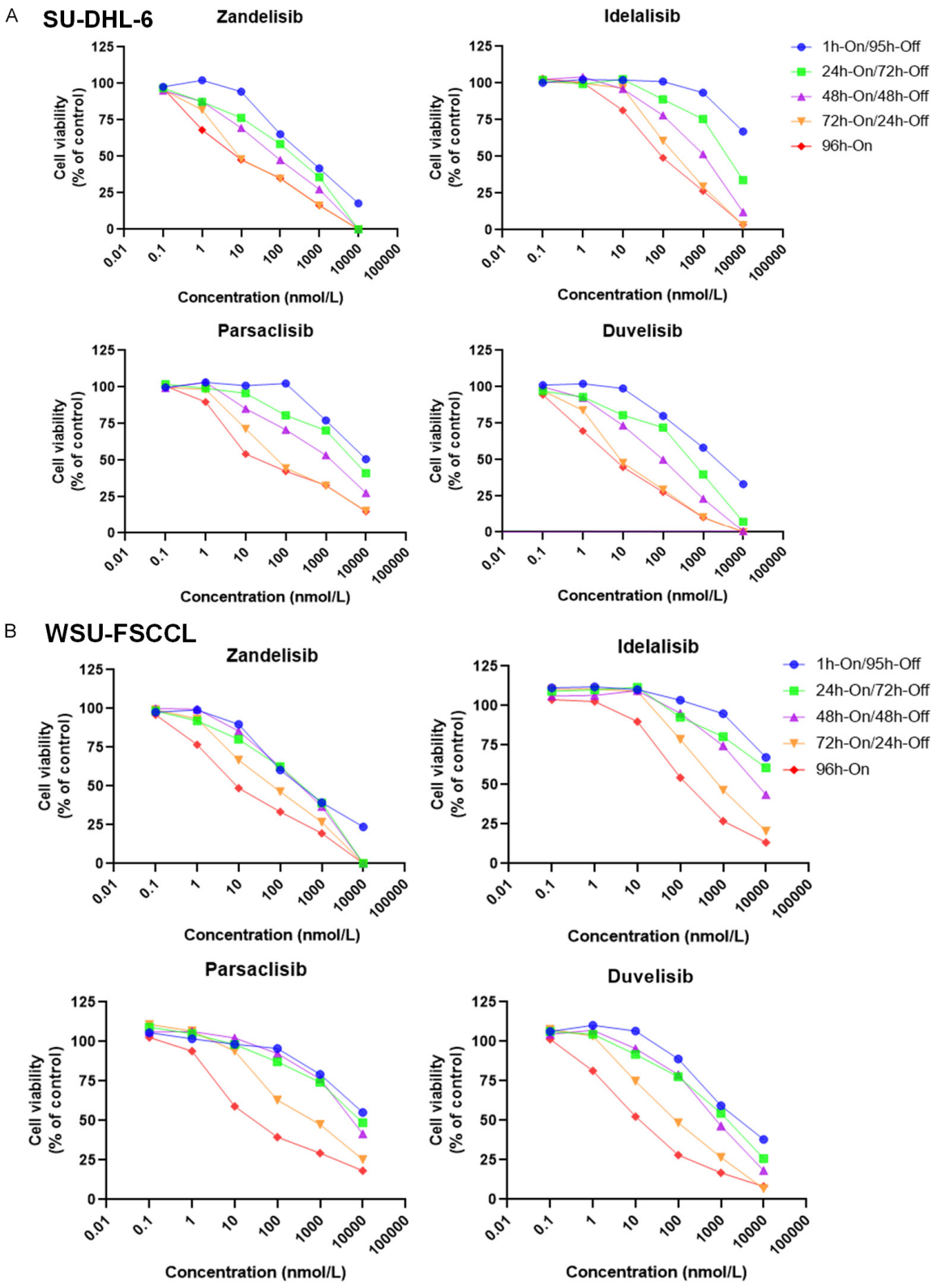

Figure 5. Inhibitory activity of zandelisib, idelalisib, parsaclisib, and duvelisib on the viability of SU-DHL-6 cells and WSU-FSCCL cells. (A) SU-DHL-6 cells and (B) WSU-FSCCL cells were treated with zandelisib, idelalisib, parsaclisib, or duvelisib for 1, 24, 48, 72, or 96 hours followed by additional 95, 72, 48, 24, or 0 hours drug-free periods. Cell viability was measured 96 hours after the start of the test compounds treatment. Each plot shows the mean values for each condition.

Table 3. IC_{50} values in SU-DHL-6 cells

IC_{50} (nmol/L)	Experimental condition				
	1 hour-on/95 hour-off	24 hour-on/72 hour-off	48 hour-on/48 hour-off	72 hour-on/24 hour-off	96 hour-on
Zandelisib	420	260	95	15	9.2
Idelalisib	> 10000	5000	1000	240	120
Parsaclisib	9900	5400	1200	76	37
Duvelisib	1800	530	100	13	6.6

Table 4. IC_{50} values in WSU-FSCCL cells

IC_{50} (nmol/L)	Experimental condition				
	1 hour-on/95 hour-off	24 hour-on/72 hour-off	48 hour-on/48 hour-off	72 hour-on/24 hour-off	96 hour-on
Zandelisib	270	380	340	82	11
Idelalisib	> 10000	> 10000	5800	700	140
Parsaclisib	> 10000	9300	6400	510	29
Duvelisib	2100	1500	790	95	13

creased at 0.5, 2, 4, and 8 hours after administration of 50 mg/kg zandelisib. The decrease seemed more pronounced at 100 mg/kg than at 50 mg/kg (**Figure 6C**).

The *in vivo* anti-tumor activity of zandelisib was evaluated in the SU-DHL-6 s.c. xenograft model. Significant tumor growth inhibition was observed in the group treated with 100 mg/kg zandelisib treated group compared to control treated mice (**Figure 6D**).

Crystal structure of PI3Kδ in complex with zandelisib

We determined the PI3Kδ structure in complex with zandelisib at 2.5 Å resolution. Data collection and refinement statistics of the structure are described in Supplementary Tables 1 and 2. The binding pocket for zandelisib of p110δ was shown in **Figure 7**. Zandelisib adopted a propeller-shaped conformation (two roughly orthogonally oriented ring systems) like other propeller-shaped inhibitors [22]. Zandelisib formed the three characteristic interactions with p110δ: the phenyl group of zandelisib formed van der Waals interactions with Met752 and Trp760 in p110δ, the methylpiperizine group of zandelisib formed hydrophobic interactions with the exposed surface of Trp760, known as the p110δ tryptophan shelf [23], the nitrogen atom of the benzimidazole group of zandelisib formed a hydrogen bond with the side chain of Lys779 in p110δ. Zandelisib has a large size scaffold (**Figure 1**) and is involved in many hydrophobic interactions with the surrounding residue in p110δ, with a maximum distance of 4.0 Å: Met752, Pro758, Trp760, Ile777, Tyr813, Ile825, Val827, Val828, Met900, Ile910. These interactions occurred in a manner that occupied the hydrophobic regions I and II, which are observed in protein kinases.

Discussion

PI3Kδ inhibitors are beneficial in the treatment of B cell malignancies. However, the use of PI3Kδ inhibitors in clinical practice is limited by their associated immune-mediated adverse events, which may be caused by the on-target suppression of regulatory T cells [24, 25]. The intermittent dosing regimen of zandelisib was designed to minimize regulatory T cell reduction and minimize immune-mediated toxicity. Indeed, the intermittent dosing regimen of zandelisib reduced the incidence of side effects while maintaining therapeutic efficacy compared to continuous dosing regimen [13, 14]. It has been shown that dissociation of zandelisib from PI3Kδ protein is slow, and zandelisib is readily transferred from the blood to the tumor, suggesting that these properties of zandelisib may contribute to its efficacy in intermittent dosing regimens [17]. We focused on the long-lasting properties of zandelisib and conducted studies, which demonstrated that the binding mode of zandelisib might contribute to its sustained characteristics as a PI3Kδ inhibitor.

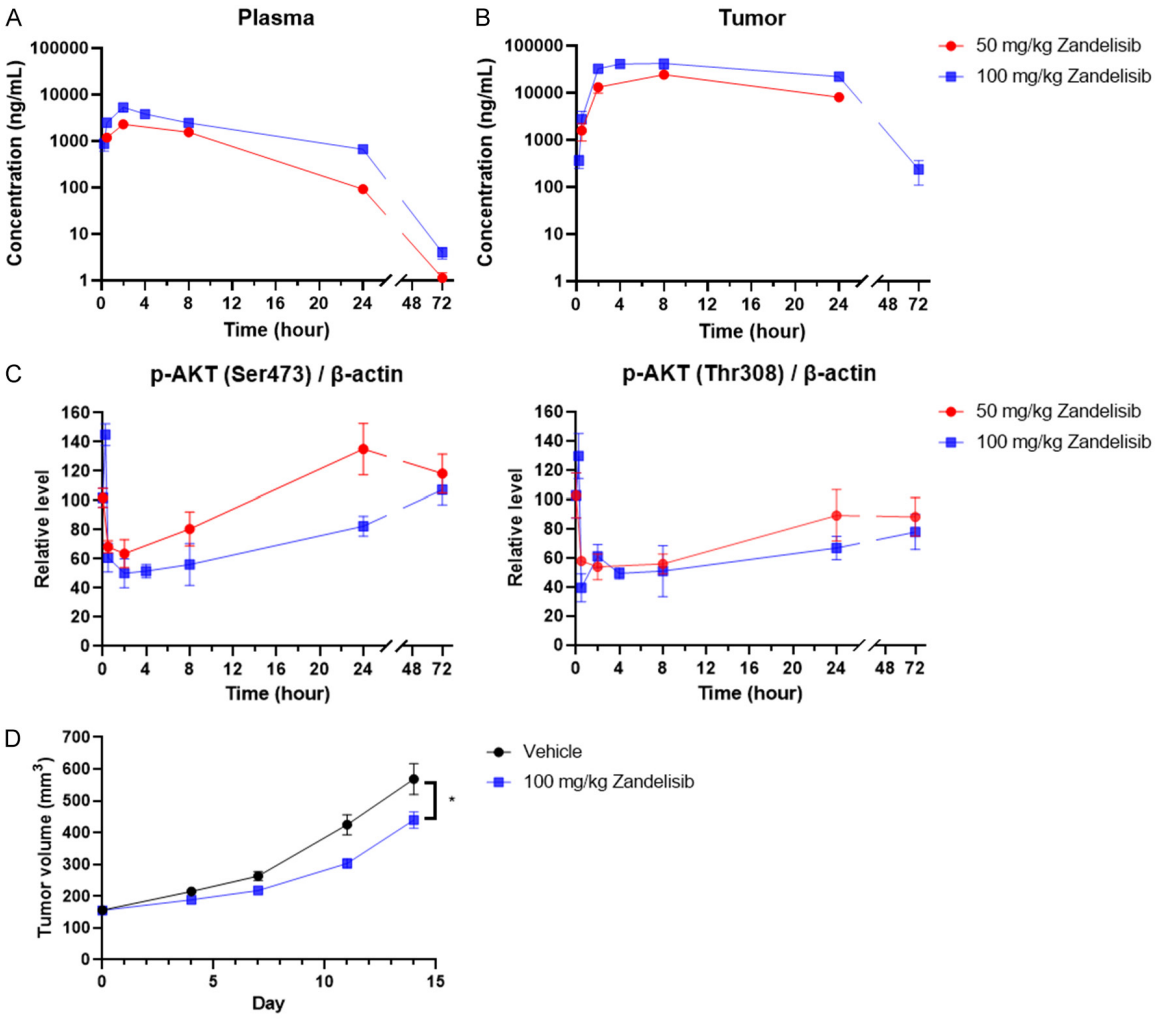

Figure 6. PK/PD relationships and anti-tumor effect of zandelisib in a mouse xenograft model of SU-DHL-6. Zandelisib (50 or 100 mg/kg) was administered once orally to SU-DHL-6 tumor bearing mouse, and (A) the plasma and (B) the tumors were collected 0.25, 0.5, 2, 4, 8, 24, or 72 hours after the administration. The plasma and intratumor concentrations of zandelisib were measured. N = 3/timepoint for the 50 mg/kg group and n = 4/time point for the 100 mg/kg group. Red circles and blue squares indicate mean values, and error bars indicate standard devistions for each group. (C) The levels of p-AKT (Ser473), p-AKT (Thr308), and β-actin were evaluated by western blotting. The relative level of p-AKT (Ser473) and p-AKT (Thr308) corrected with β-actin was calculated and plotted against time. Red circles and blue squares indicate mean values, and error bars indicate standard errors for each group. (D) Anti-tumor activity was measured. Vehicle or zandelisib (100 mg/kg) was administered orally once daily from days 0 to 13. Mean ± standard error are shown. N = 15. *: $p<0.05$.

Table 5. PK parameter in plasma samples

Dose (mg/kg)	t_{max} (h)	C_{max} (ng/mL)	AUC_{0-t} (ng·h/mL)	$AUC_{0-\infty}$ (ng·h/mL)	$t_{1/2}$ (h)
50	2	2290	29800	29800	6.42
100	2	5330	69000	69000	6.87

In the present study, we evaluated the binding mode and the pharmacological effects of zandelisib compared with other PI3Kδ inhibitors (idelalisib, parsaclisib, and duvelisib). In SPR analysis using the Biacore™ system, zandelisib showed the lowest dissociation rate among the four compounds. Despite the relatively close K_D values for duvelisib and zandelisib, a significant difference in residence time was observed. While K_D reflects a compound's affinity for its target, residence time is influenced not only by affinity but also by the kinetics of bind-

Table 6. PK parameter in tumor samples

Dose (mg/kg)	t_{max} (h)	C_{max} (ng/g)	AUC_{0-t} (ng·h/g)	$AUC_{0-\infty}$ (ng·h/g)	$t_{1/2}$ (h)
50	8	24200	381000	NC	NC
100	8	42000	1310000	NC	NC

Zandelisib was orally administered at doses of 50 (n = 3/timepoint) and 100 mg/kg (n = 4/timepoint) to SCID mouse bearing SU-DHL-6. NC: not calculated.

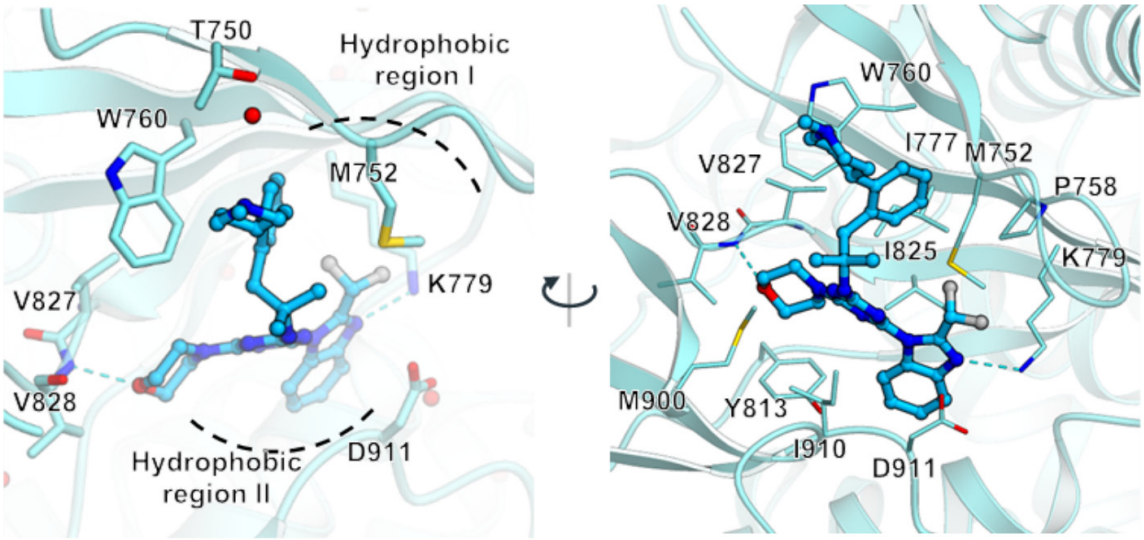

Figure 7. Binding pocket for zandelisib on p110δ. Zandelisib is shown as ball-and-stick and key residues in p110δ for zandelisib binding are shown as sticks. Water molecules are shown as red balls. Dashed lines indicate hydrogen-bonding interactions. Zandelisib formed hydrogen bonds with the main chain of Val828 and the side chain of Lys779.

ing and dissociation. It was suggested that the slower dissociation of zandelisib contributes to the difference in residence time, allowing it to remain bound to the target for an extended period. Indeed, re-injection of the same compounds after a dissociation period in the SPR analysis showed that zandelisib had nearly irreversible binding properties. Even with similar K_D values, this difference in residence time may lead to prolonged pharmacological effects. This slow dissociation characteristic of zandelisib was also observed in living cells using the BRET assay, where zandelisib dissociated slowly like the covalent irreversible inhibitor wortmannin. It has been reported that wortmannin is unstable in biological fluids [26]. Its unstable characteristics may contribute to its shorter residence time compared to zandelisib. In the wash-out experiments using B cell lines, idelalisib, parsaclisib, and duvelisib completely lost their PI3Kδ inhibitory activity, and their cell proliferation inhibitory activity was also considerably reduced once they were washed out. On the other hand, zandelisib maintained its PI3Kδ inhibitory activity and its cell proliferation inhibitory activity after washout. These results could be explained by the dissociation rate or reversibility of each test compound from PI3Kδ. Indeed, the concentration of zandelisib in the cells after washout was higher than that of the other compounds. In *in vivo* experiments, as previously reported by Moreno et al., the distribution of zandelisib after administration was higher in the tumor than in the blood; at 50 mg/kg it continued to inhibit PI3Kδ for 8 hours and at 100 mg/kg for 24 hours in the tumors, confirming its long-lasting PI3Kδ inhibitory effect. Consistent with these findings, zandelisib showed significant anti-tumor activity in the tumor bearing mouse model.

To obtain mechanistic insights into the long-lasting property of zandelisib in PI3Kδ inhibition, we revealed the binding mode of zandelisib to p110δ by X-ray crystallography. As previously reported, the propeller-shaped geome-

try is known to intrinsically impart PI3Kδ selectivity to ligands by inducing the formation of the specificity pocket and the tryptophan shelf [27]. Zandelisib adopted the propeller-shaped conformation (**Figure 7**) and bound to p110δ in a manner that occupied the tryptophan shelf (Supplementary Figure 2) like the other p110δ-selective inhibitors. This binding mode of zandelisib could explain its high p110δ selectivity.

Comparison of the ligand binding site of PI3K in complex with zandelisib and other PI3K inhibitors [28, 29] in Supplementary Figure 3 revealed that idelalisib formed a water-mediated hydrogen bond network with Asp911 in p110δ (Supplementary Figure 3A). This interaction occurred within a hydrophilic environment of the binding pocket. In contrast, zandelisib excluded these water molecules and formed a hydrogen bond with Lys779 in p110δ while shielding the binding pocket from water. Lys779 has been reported as the binding site for covalent interaction with irreversible inhibitors of PI3Kδ [30, 31], including wortmannin (Supplementary Figure 3B). In general, water-shielded hydrogen bonds are known to enhance the kinetic stability of protein-ligand complexes [32]. It was suggested that the binding mode of zandelisib may contribute to slow dissociation properties. Moreover, zandelisib formed hydrophobic interactions with p110δ, containing 11 hydrophobic residues within approximately 4 Å. The large occupied surface area in the binding pocket compared to other inhibitors may contribute to the slow dissociation rate of zandelisib.

Overall, those data suggest that the binding mode of zandelisib to PI3Kδ not only contribute to the high selectivity for PI3Kδ, but also to the prolonged PI3Kδ residence time, resulting in the sustained pharmacological effects.

Conclusion

The current studies revealed that zandelisib has distinct properties compared to the other PI3Kδ inhibitors in terms of pharmacological activities and binding mode. These properties may differentiate zandelisib from other inhibitors in terms of clinical efficacy.

Acknowledgements

We thank Yuko Takashima, Kumiko Masunaga, Etsuko Koshimura, Satomi Nagata, Kozue Higuchi, Miyoko Asano, Yoko Hasegawa-Yoda, Shigeru Hirose, and Daisuke Yamaguchi (Kyowa Kirin Co., Ltd.) for supporting the studies. We thank Sandy Wiley (MEI Pharma Inc., San Diego, CA, USA) for supporting this research and reviewing this article.

Disclosure of conflict of interest

Kana Kunieda, Chisae Nagiri, Miwa Watanabe, Tadashi Yoshida, Jian Zou, Ayumi Kaneda, Yuichi Takahashi, Kenichi Aburai, Jun-ichi Saito, Hiroshi Umehara, Yoshiaki Otsu, Toshihiko Ishii are employees of Kyowa Kirin Co., Ltd.

Address correspondence to: Kana Kunieda, Research Division, Kyowa Kirin Co., Ltd., 1188, Shimotogari, Nagaizumi-cho, Sunto-gun, Shizuoka, Japan. E-mail: kana.kunieda.vh@kyowakirin.com

References

[1] Whyte DB and Holbeck SL. Correlation of PIK-3Ca mutations with gene expression and drug sensitivity in NCI-60 cell lines. Biochem Biophys Res Commun 2006; 340: 469-475.
[2] Manning BD and Toker A. AKT/PKB signaling: navigating the network. Cell 2017; 169: 381-405.
[3] Tzenaki N and Papakonstanti EA. p110δ PI3 kinase pathway: emerging roles in cancer. Front Oncol 2013; 3: 40.
[4] Jellusova J and Rickert RC. The PI3K pathway in B cell metabolism. Crit Rev Biochem Mol Biol 2016; 51: 359-378.
[5] Puri KD and Gold MR. Selective inhibitors of phosphoinositide 3-kinase delta: modulators of B-cell function with potential for treating autoimmune inflammatory diseases and B-cell malignancies. Front Immunol 2012; 3: 256.
[6] Hoellenriegel J, Meadows SA, Sivina M, Wierda WG, Kantarjian H, Keating MJ, Giese N, O'Brien S, Yu A, Miller LL, Lannutti BJ and Burger JA. The phosphoinositide 3'-kinase delta inhibitor, CAL-101, inhibits B-cell receptor signaling and chemokine networks in chronic lymphocytic leukemia. Blood 2011; 118: 3603-3612.
[7] Lannutti BJ, Meadows SA, Herman SE, Kashishian A, Steiner B, Johnson AJ, Byrd JC, Tyner JW, Loriaux MM, Deininger M, Druker BJ, Puri KD, Ulrich RG and Giese NA. CAL-101, a p110delta selective phosphatidylinositol-3-kinase inhibitor for the treatment of B-cell malignancies, inhibits PI3K signaling and cellular viability. Blood 2011; 117: 591-594.
[8] Gopal AK, Kahl BS, de Vos S, Wagner-Johnston ND, Schuster SJ, Jurczak WJ, Flinn IW, Flowers CR, Martin P, Viardot A, Blum KA, Goy AH, Da-

vies AJ, Zinzani PL, Dreyling M, Johnson D, Miller LL, Holes L, Li D, Dansey RD, Godfrey WR and Salles GA. PI3Kδ inhibition by idelalisib in patients with relapsed indolent lymphoma. N Engl J Med 2014; 370: 1008-1018.
[9] Yu M, Chen J, Xu Z, Yang B, He Q, Luo P, Yan H and Yang X. Development and safety of PI3K inhibitors in cancer. Arch Toxicol 2023; 97: 635-650.
[10] Lawrence L. PI3K inhibitors: a series of unfortunate events. 2023.
[11] Matthews D, O'Farrell M, Ventura R, Brown SD and Tai A. Discovery of PI3K delta inhibitors for the treatment of inflammatory and autoimmune disease. CAL 2012; 101: 3-9.
[12] O'Farrell M, Ventura R, Tai A, Tyner JW, Loriaux MM, Mahadevan D, Morales C, Brown SD and Matthews DJ. Preclinical characterization of PWT143, a novel selective and potent phosphatidylinositol 3-kinase delta (PI3K delta) inhibitor with ex-vivo activity in hematologic malignancies. Blood 2012; 120: 2907.
[13] Pagel JM, Soumerai JD, Reddy N, Jagadeesh D, Stathis A, Asch A, Salman H, Kenkre VP, Iasonos A, Llorin-Sangalang J, Li J and Zelenetz AD. Zandelisib with continuous or intermittent dosing as monotherapy or in combination with rituximab in patients with relapsed or refractory B-cell malignancy: a multicentre, first-in-patient, dose-escalation and dose-expansion, phase 1b trial. Lancet Oncol 2022; 23: 1021-1030.
[14] Zelenetz AD, Jurczak W, Ribrag V, Linton K, Collins GP, Jiménez JL, Bishton M, Dholaria B, Mengarelli A, Phillips TJ, Sungala N, Musuraca G, Sheehy O, Van Den Neste E, Odera M, Miao L, Gold DP, Ghalie RG and Zinzani PL. The PI3Kδ inhibitor zandelisib on intermittent dosing in relapsed/refractory follicular lymphoma: Results from a global phase 2 study. Hemasphere 2024; 8: e138.
[15] Goto H, Izutsu K, Ennishi D, Mishima Y, Makita S, Kato K, Hanaya M, Hirano S, Narushima K, Teshima T, Nagai H and Ishizawa K. Zandelisib (ME-401) in Japanese patients with relapsed or refractory indolent non-Hodgkin's lymphoma: an open-label, multicenter, dose-escalation phase 1 study. Int J Hematol 2022; 116: 911-921.
[16] Munakata W, Kumode T, Goto H, Fukuhara N, Shimoyama T, Takeuchi M, Kawakita T, Kubo K, Sawa M, Uchida T, Mishima Y, Ichii M, Hanaya M, Matsumoto A, Kuriki M, Seike T, Izutsu K and Ishizawa K. A phase II study of zandelisib in patients with relapsed or refractory indolent non-Hodgkin lymphoma: ME-401-K02 study. Br J Haematol 2025; 206: 541-550.
[17] Moreno O and Wood J. Absorption, distribution, and binding profile of ME-401, a potent and selective oral small-molecule inhibitor of phosphatidylinositol 3-kinase δ (PI3Kδ) in animal and B-cell lymphoma models. Target Oncol 2019; 14: 603-611.
[18] Skånland SS and Brown JR. PI3K inhibitors in chronic lymphocytic leukemia: where do we go from here? Haematologica 2023; 108: 9-21.
[19] Robers MB, Dart ML, Woodroofe CC, Zimprich CA, Kirkland TA, Machleidt T, Kupcho KR, Levin S, Hartnett JR, Zimmerman K, Niles AL, Ohana RF, Daniels DL, Slater M, Wood MG, Cong M, Cheng YQ and Wood KV. Target engagement and drug residence time can be observed in living cells with BRET. Nat Commun 2015; 6: 10091.
[20] Packeu A, Wennerberg M, Balendran A and Vauquelin G. Estimation of the dissociation rate of unlabelled ligand-receptor complexes by a 'two-step' competition binding approach. Br J Pharmacol 2010; 161: 1311-1328.
[21] Castanedo GM, Blaquiere N, Beresini M, Bravo B, Brightbill H, Chen J, Cui HF, Eigenbrot C, Everett C, Feng J, Godemann R, Gogol E, Hymowitz S, Johnson A, Kayagaki N, Kohli PB, Knüppel K, Kraemer J, Krüger S, Loke P, McEwan P, Montalbetti C, Roberts DA, Smith M, Steinbacher S, Sujatha-Bhaskar S, Takahashi R, Wang X, Wu LC, Zhang Y and Staben ST. Structure-based design of tricyclic NF-κB inducing kinase (NIK) inhibitors that have high selectivity over phosphoinositide-3-kinase (PI3K). J Med Chem 2017; 60: 627-640.
[22] Vanhaesebroeck B, Perry MWD, Brown JR, André F and Okkenhaug K. PI3K inhibitors are finally coming of age. Nat Rev Drug Discov 2021; 20: 741-769.
[23] Sutherlin DP, Baker S, Bisconte A, Blaney PM, Brown A, Chan BK, Chantry D, Castanedo G, DePledge P, Goldsmith P, Goldstein DM, Hancox T, Kaur J, Knowles D, Kondru R, Lesnick J, Lucas MC, Lewis C, Murray J, Nadin AJ, Nonomiya J, Pang J, Pegg N, Price S, Reif K, Safina BS, Salphati L, Staben S, Seward EM, Shuttleworth S, Sohal S, Sweeney ZK, Ultsch M, Waszkowycz B and Wei B. Potent and selective inhibitors of PI3Kδ: obtaining isoform selectivity from the affinity pocket and tryptophan shelf. Bioorg Med Chem Lett 2012; 22: 4296-4302.
[24] Chellappa S, Kushekhar K, Munthe LA, Tjønnfjord GE, Aandahl EM, Okkenhaug K and Taskén K. The PI3K p110δ isoform inhibitor idelalisib preferentially inhibits human regulatory T cell function. J Immunol 2019; 202: 1397-1405.
[25] Hanlon A and Brander DM. Managing toxicities of phosphatidylinositol-3-kinase (PI3K) inhibitors. Hematology Am Soc Hematol Educ Program 2020; 2020: 346-356.

[26] Yuan H, Barnes KR, Weissleder R, Cantley L and Josephson L. Covalent reactions of wortmannin under physiological conditions. Chem Biol 2007; 14: 321-328.
[27] Williams R, Berndt A, Miller S, Hon WC and Zhang X. Form and flexibility in phosphoinositide 3-kinases. Biochem Soc Trans 2009; 37: 615-626.
[28] Somoza JR, Koditek D, Villaseñor AG, Novikov N, Wong MH, Liclican A, Xing W, Lagpacan L, Wang R, Schultz BE, Papalia GA, Samuel D, Lad L and McGrath ME. Structural, biochemical, and biophysical characterization of idelalisib binding to phosphoinositide 3-kinase δ. J Biol Chem 2015; 290: 8439-8446.
[29] Walker EH, Pacold ME, Perisic O, Stephens L, Hawkins PT, Wymann MP and Williams RL. Structural determinants of phosphoinositide 3-kinase inhibition by wortmannin, LY294002, quercetin, myricetin, and staurosporine. Mol Cell 2000; 6: 909-919.
[30] Dalton SE, Dittus L, Thomas DA, Convery MA, Nunes J, Bush JT, Evans JP, Werner T, Bantscheff M, Murphy JA and Campos S. Selectively targeting the kinome-conserved lysine of PI3Kδ as a general approach to covalent kinase inhibition. J Am Chem Soc 2018; 140: 932-939.
[31] Fournier JCL, Evans JP, Zappacosta F, Thomas DA, Patel VK, White GV, Campos S and Tomkinson NCO. Acetylation of the catalytic lysine inhibits kinase activity in PI3Kδ. ACS Chem Biol 2021; 16: 1644-1653.
[32] Schmidtke P, Luque FJ, Murray JB and Barril X. Shielded hydrogen bonds as structural determinants of binding kinetics: application in drug design. J Am Chem Soc 2011; 133: 18903-18910.

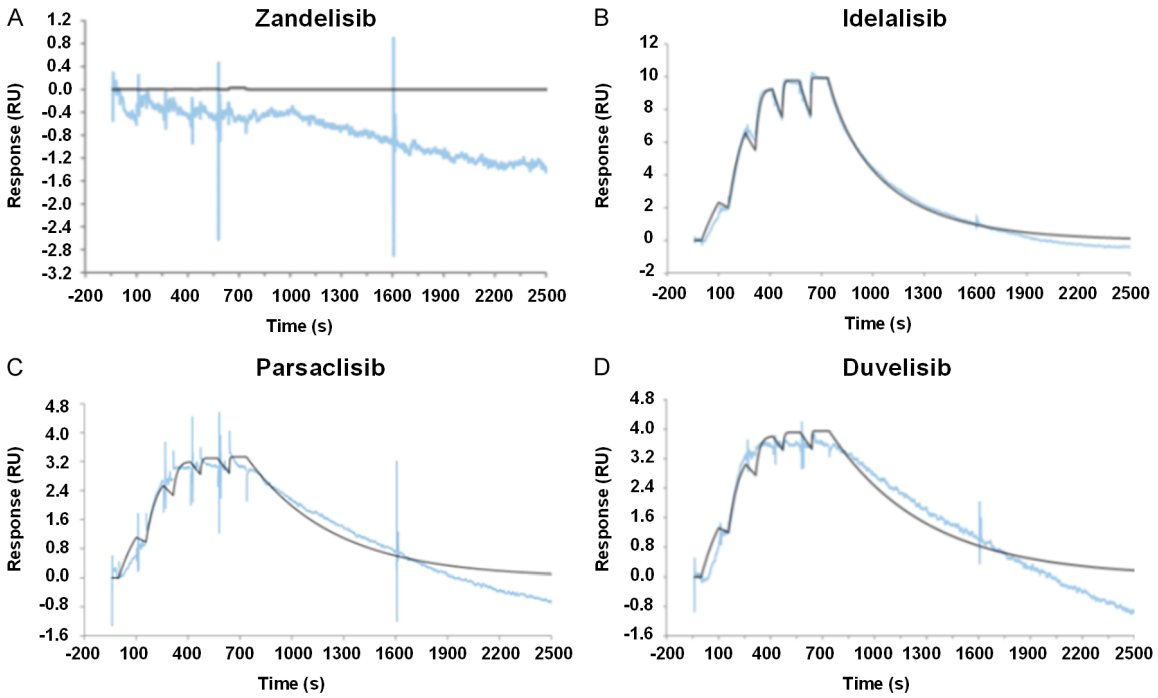

Supplementary Figure 1. The second mesurement of single cycle kinetic curves of zandelisib, idelalisib, parsaclisib, or duvelisib on PI3Kδ. After the first single cycle kinetic assay of (A) 1-100 nmol/L zandelisib, (B) 1-100 nmol/L idelalisib, (C) 1-100 nmol/L parsaclisib, and (D) 1-100 nmol/L duvelisib on PI3Kδ, the same compound was injected and measured again in the same concentration range. These assays were performed in duplicate. N = 1 data are shown. The blue line shows the sensorgram before fitting and the black line shows the sensorgram after fitting by Biacore™ 8K control Software.

Supplementary Table 1. Data collection statistics of zandelisib-bound PI3Kδ crystal

Space group	$P2_12_12_1$
Cell dimensions	
a, b, c (Å)	90.89, 109.08, 142.44
α, β, γ (°)	90, 90, 90
Resolution (Å)	45.45-2.50 (2.58-2.50)
R_{merge} (%)	4.1 (119.3)
R_{meas} (%)	4.5 (129.6)
R_{pim} (%)	1.7 (49.9)
No. of observations	334,446 (30,244)
No. of unique observations	49,670 (4,525)
$I/\sigma(I)$	18.7 (1.6)
$CC_{1/2}$	1.000 (0.858)
Completeness (%)	99.9 (99.7)
Redundancy	6.7 (6.7)

Values in parentheses are for the outer shell.

Supplementary Table 2. Refinement statistics of zandelisib-bound PI3Kδ structure

Resolution (Å)	45.45-2.50 (2.55-2.50)
No. of reflections used	49,577 (2,871)
R_{work}/R_{free} (%)	23.0/27.8 (37.7/43.8)
No. of atoms	
Protein	8,847
Zandelisib	42
Water	49
B-factors	
Protein	97.3
Zandelisib	82.5
Water	86.8
R.m.s deviations	
Bond length (Å)	0.003
Bond angles (°)	0.559
Ramachandran statistics	
Favored (%)	96.4
Allowed (%)	3.5
Disallowed (%)	0.1

Values in parentheses are for the outer shell.

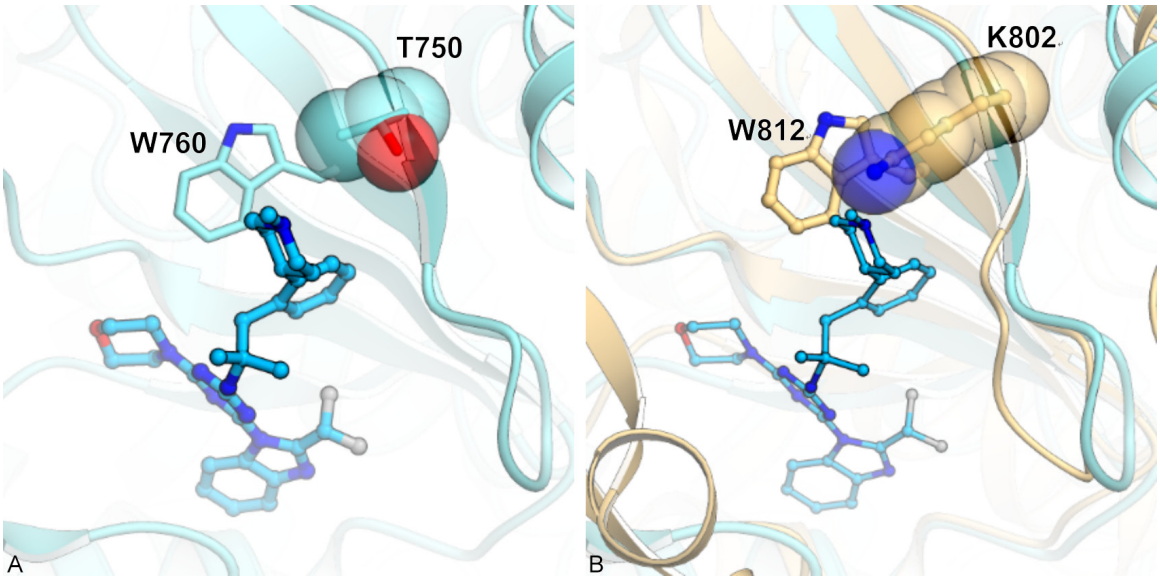

Supplementary Figure 2. Comparison of the tryptophan region for crystal structures of p110δ and p110γ. (A) Tryptophan shelf is formed by Trp760 and Thr750 for p110δ in complex with zandelisib, and (B) superimposition of Trp812 and Lys802 in pig p110γ (PDB ID: 1E7U, colored as orange, wortmannin is not shown) equivalent to Trp760 and Thr750 in p110δ. Lys802 in p110γ is sterically clashed with zandelisib in p110δ.

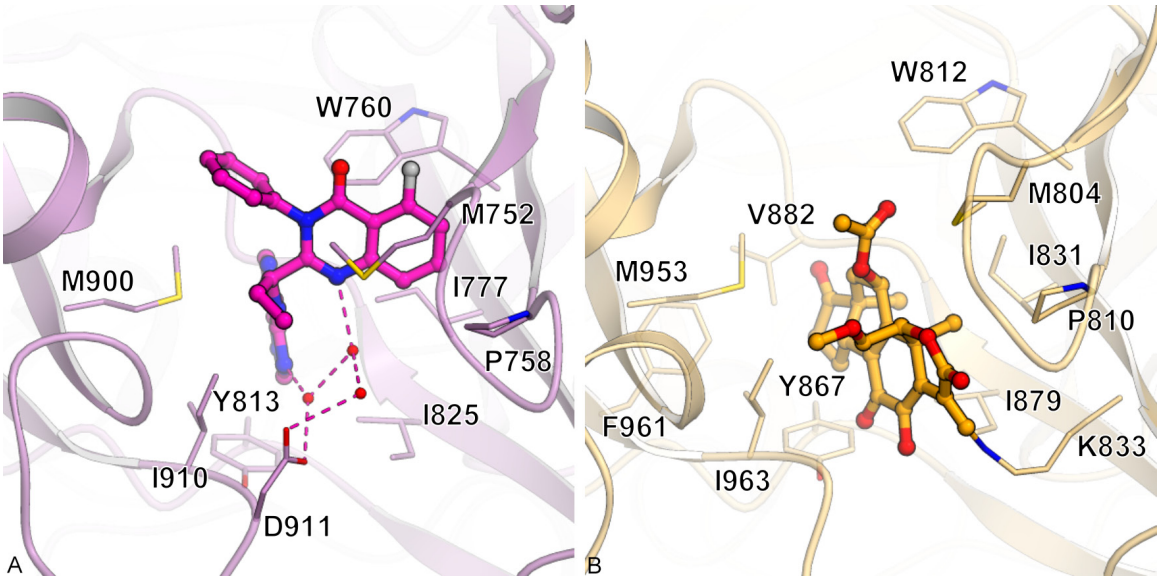

Supplementary Figure 3. Comparison of the ligand binding pocket of PI3K. (A) Idelalisib bound to mouse p110δ (PDB ID: 4XE0, colored as magenta) and (B) wortmannin covalently bound to p110γ (PDB ID: 1E7U, colored as orange), with the residues within a maximum distance of 4 Å in the vicinity in zandelisib. Each ligand is shown as a ball and stick model and p110δ and p110γ are shown as ribbon models. Water molecules are shown as red balls. Dashed lines indicate hydrogen-bonding interactions.